European Journal of Radiology Open 13 (2024) 100588

Contents lists available at ScienceDirect

European Journal of Radiology Open

journal homepage: www.elsevier.com/locate/ejro

Enhancing the image quality of prostate diffusion-weighted imaging in patients with prostate cancer through model-based deep learning reconstruction

Noriko Nishioka [a,b], Noriyuki Fujima [a,*], Satonori Tsuneta [a,c], Masato Yoshikawa [a], Rina Kimura [a,b], Keita Sakamoto [a], Fumi Kato [a,d], Haruka Miyata [e], Hiroshi Kikuchi [e], Ryuji Matsumoto [e], Takashige Abe [e], Jihun Kwon [f], Masami Yoneyama [f], Kohsuke Kudo [a,b,g]

[a] Department of Diagnostic and Interventional Radiology, Hokkaido University Hospital, N14 W5, Kita-Ku, Sapporo 060-8648, Japan
[b] Department of Diagnostic Imaging, Faculty of Medicine and Graduate School of Medicine, Hokkaido University, N15 W7, Kita-ku, Sapporo 060-8638, Japan
[c] Department of Radiology, Graduate School of Dental Medicine, Hokkaido University, N13 W7, Kita-ku, Sapporo 060-8586, Japan
[d] Department of Radiology, Jichi Medical University Saitama Medical Center, 1-847 Amanuma-cho, Omiya-ku, Saitama, 330-8503, Japan
[e] Department of Renal and Genitourinary Surgery, Faculty of Medicine and Graduate School of Medicine, Hokkaido University, N15 W7, Kita-Ku, Sapporo 060-8638, Japan
[f] Philips Japan Ltd., 1-3-1 Azabudai, Minato-ku, Tokyo 106-0041, Japan
[g] Global Center for Biomedical Science and Engineering, Faculty of Medicine, Hokkaido University, N14 W5, Kita-Ku, Sapporo, 060-8648, Japan

HIGHLIGHTS

- Diffusion-weighted imaging (DWI) is vital for prostate cancer detection in MRI.
- Model-based deep learning reconstruction was applied for prostate DWI (DL-DWI).
- DL-DWI improved both qualitative and quantitative aspects of the image quality.

ARTICLE INFO

Keywords:
Prostate
DWI
Deep learning reconstruction
Image quality

ABSTRACT

Purpose: To evaluate the utility of model-based deep learning reconstruction in prostate diffusion-weighted imaging (DWI).

Methods: This retrospective study evaluated two prostate diffusion-weighted imaging (DWI) methods: deep learning reconstruction (DL-DWI) and traditional parallel imaging (PI-DWI). We examined 32 patients with radiologically diagnosed and histologically confirmed prostate cancer (PCa) lesions ≥10 mm. Image quality was evaluated both qualitatively (for overall quality, prostate conspicuity, and lesion conspicuity) and quantitatively, using the signal-to-noise ratio (SNR), contrast-to-noise ratio (CNR), and apparent diffusion coefficient (ADC) for prostate tissue.

Results: In the qualitative evaluation, DL-DWI scored significantly higher than PI-DWI for all three parameters ($p<0.0001$). In the quantitative analysis, DL-DWI showed significantly higher SNR and CNR values compared to PI-DWI ($p<0.0001$). Both the prostate tissue and the lesions exhibited significantly higher ADC values in DL-DWI compared to PI-DWI ($p<0.0001$, $p=0.0014$, respectively).

Conclusion: Model-based DL reconstruction enhanced both qualitative and quantitative aspects of image quality in prostate DWI. However, this study did not include comparisons with other DL-based methods, which is a limitation that warrants future research.

* Correspondence to: Department of Diagnostic and Interventional Radiology, Hokkaido University Hospital, N14 W5, Kita-Ku, Sapporo, Hokkaido 060-8648, Japan.
E-mail address: fujima@med.hokudai.ac.jp (N. Fujima).

https://doi.org/10.1016/j.ejro.2024.100588
Received 13 May 2024; Received in revised form 16 June 2024; Accepted 30 June 2024

1. Introduction

Multiparametric magnetic resonance imaging (mp-MRI) plays a crucial role in the diagnosis of prostate cancer (PCa) by enabling its detection, localization, and staging [1]. Among the mp-MRI sequences, T2-weighted imaging (T2WI) and diffusion-weighted imaging (DWI) are particularly important when scoring lesions based on the Prostate Imaging Reporting and Data System (PI-RADS). With the revision of the PI-RADS from version 2 to version 2.1, the significance of DWI in the categorization of lesions was further increased [2,3].

The single-shot spin-echo echo-planar imaging (EPI) sequence is the most commonly used technique in clinical DWI; however, it suffers from geometric image distortion, which can adversely affect the diagnostic performance. Combining single-shot spin-echo EPI with parallel imaging (PI) techniques [4] reduces this distortion. However increasing the reduction factor with PI decreases the signal-to-noise ratio (SNR), particularly in regions with high geometric (g-)factors such as the central part of the image [5,6]. In addition, the high b-values recommended in PI-RADS ver. 2.1 [2,3] often result in an insufficient SNR in prostate DWI. Effective noise reduction methods are thus highly desired to overcome these issues.

Convolutional neural network (CNN)-based deep learning (DL) has shown promising results for MRI image reconstruction [7,8]. Among the DL-based techniques, the "model-based" processes have proven effective for MRI image-denoising in various anatomical regions, including the knee [9], ankle [10], coronary artery [11], breast [12], and neck [13]. These studies applied a model-based approach using the deep-learning architecture of adaptive compressed-sensing sensitivity-encoding (CS)-Net (Adaptive-CS-Net), replacing the wavelet transform in conventional compressed sensing algorithms with a CNN-based approach. The majority of previously studied DL-based techniques are known as "end-to-end-type" DL reconstruction. This type of reconstruction typically focuses on the output image only in its reconstruction process. In contrast, model-based DL reconstruction integrates the CNN into the image reconstruction cycle. Consequently, unlike the end-to-end approach that processes only the output image, the model-based DL reconstruction method is expected to effectively manage large amounts of signal data throughout the image reconstruction process. As a result, this model-based DL technique holds promise for efficiently removing noise in DWI and is expected to provide effective denoising in challenging imaging scenarios. To the best of our knowledge, there has been no investigation into the use of model-based DL reconstruction for prostate DWI, and its effectiveness remains unknown. It is important to assess the extent to which model-based DL reconstruction can improve image quality in prostate DWI.

We conducted the present study to evaluate the utility of model-based DL reconstruction in prostate DWI by comparing it with conventional PI-based reconstruction images.

2. Patients and methods

2.1. Patients

A total of 79 patients were referred to our hospital for a prostate evaluation and underwent MR scanning during the period June 3, 2022 through January 31, 2023. From among these 79 patients, we selected the cases of 32 patients who met all of the following four inclusion criteria: (1) they were examined by prostate mp-MRI on a specific MR scanner equipped with the DL-based reconstruction function, (2) their MRI dataset including DWI with both the conventional PI- and DL-based reconstructions was available, (3) the patients' radiology reports demonstrated marked hyperintensity on DWI and focal marked hypointensity on an apparent diffusion coefficient (ADC) map sized $\geq$10 mm (i.e., PI-RADS ver. 2.1, DWI score 4 or 5 points), and (4) the patients had undergone a radical prostatectomy and/or transrectal prostate biopsy, and the presence of PCa in a location consistent with the images was confirmed. If the pathologic evaluation was based on tissue obtained from a transrectal prostate biopsy, inclusion in the study required that (*i*) an MRI-US (ultrasound) fusion-guided targeted biopsy had been performed on the site where the lesion was identified by imaging, or (*ii*) if a targeted biopsy was not performed due to the large size of the lesion, PCa was confirmed across multiple cores by a systematic biopsy.

This retrospective study was approved by our hospital's institutional review board, and the requirement for patients' written informed consent was waived in light of the use of anonymized patient data and the retrospective study design.

2.2. MR imaging technique

All MRI examinations were performed on a 3 T MR unit (Ingenia Elition X; Philips Healthcare, Best, the Netherlands) with a 32-channel coil (dStream Torso coil/FlexCoverage posterior coil; Philips Healthcare). The mp-MRI examinations of the prostate included axial, coronal, and sagittal T2WI, axial T1WI, two types of axial DWI (*see below*), and axial dynamic contrast-enhanced imaging. We used the findings from the patients' axial T2WI and the two types of axial DWI for the present analyses.

The acquisition parameters for the axial T2WI were as follows: repetition time (TR) 5000 ms, echo time (TE) 100 ms, flip angle (FA) 90°, field of view (FOV) 160×160 mm, reconstructed matrix 352×352 (acquired matrix 320×237), slice thickness 3 mm, and gap 0.3 mm.

Two types of DWI were separately acquired: (*i*) fat-suppressed 2D single-shot spin-echo EPI with PI reconstruction (i.e., PI-DWI), and (*ii*) fat-suppressed 2D single-shot spin-echo EPI with model-based DL reconstruction (i.e., DL-DWI). The details of the imaging parameters and the acquisition time for each type of DWI are shown in Table 1. ADC maps were calculated automatically in the MR console using b-values of 0 and 2000 s/mm^2 with a mono-exponential model.

2.3. Data processing

We used an image reconstruction model categorized as model-based DL reconstruction, with Adaptive-CS-Net based on the vendor prototype (Next Generation Scan Acceleration patch). Detailed information regarding the model training and optimization methods of Adaptive-CS-Net has been documented [9]. The technique involves iterative image processing through the Adaptive-CS-Net from an undersampled k-space dataset for effective denoising. More specifically, in the model-based DL reconstruction process, Adaptive-CS-Net replaces a portion equivalent to the wavelet transform within the compressed sensing-based image reconstruction algorithm.

Constructed with a U-Net-shaped structure and a soft thresholding function, Adaptive-CS-Net enables effective image denoising with a

Table 1
Image parameters for prostate DWI.

	PI-DWI	DL-DWI
TR, ms	5000	5000
TE, ms	61 or 73	61 or 73
FA, degrees	90	90
EPI factor	41	41
Acquired matrix	108×103	108×102
Reconstructed matrix	256×236	240×224
FOV, mm	320×295	320×299
Slice thickness, mm	3	3
Inter-slice gap, mm	0.3	0.3
Reduction factor	2.5	2.5
NEX	12	12
b-values, s/mm^2	0, 2000	0, 2000
Acquisition time, min:sec	3:15	3:15

[footnote] DL: deep learning, DWI: diffusion-weighted imaging, EPI: echo-planar imaging, FA: flip angle, FOV: field of view, NEX: number of excitations, PI: parallel imaging, TE: echo time, TR: repetition time.

sparsifying approach. This reconstruction model also uses the domain-specific prior knowledge for a data-consistency check to confirm whether or not denoising was appropriately performed by referring to the pre- and post-processed images through Adaptive-CS-Net at every point of the iterative process. Through this iterative image processing, noise and artifacts are progressively eliminated, concurrently enhancing the original signal. This ultimately leads to a substantial improvement in the quality of the image. All of these image-processing steps took place within the MR system's console. Additionally, in this study, we used a novel CNN that integrated and enhanced the Adaptive-CS-Net introduced in reference [9], with further details provided in reference [10]. In brief, the Adaptive-CS-Net was extensively pre-trained on a large dataset, using both 1.5 T and 3 T images of various anatomies and contrasts, and optimized for execution on standard reconstruction hardware, ensuring enhanced performance and applicability.

2.3.1. Image analysis: qualitative assessment

As a qualitative assessment, two board-certified radiologists with 14 and 8 years of experience in radiology, respectively, visually evaluated the PI-DWI and DL-DWI results of each patient. The evaluation focused on the following three aspects: (*i*) overall image quality, (*ii*) prostate conspicuity, and (*iii*) lesion conspicuity. Each aspect was rated using a five-point scale as follows.

Overall image quality: 1 point, the image contains excessive noise and is thus unsuitable for diagnosis; 2 points, there is significant noise in the central area, making the diagnosis challenging at times; 3 points, some noise in the central area, but the image is acceptable for diagnostic use; 4 points, slight noise, presenting minimal limitations for diagnostic use; and 5 points, hardly any noise, almost no limitations for diagnostic use.

Prostate conspicuity: 1 point, the location of the prostate cannot be identified; 2 points, the prostate is visible in part; 3 points, the outline of the prostate is about half visible; 4 points, the entire outline of the prostate is visible, but with some minor noise in the surroundings; and 5 points, the entire outline of the prostate is visible with almost no noise.

Lesion conspicuity: 1 point, the images contain excessive noise, unsuitable for diagnosis; 2 points, there is significant noise, and the signal of the lesion is obscured; 3 points, there is some noise in the center, but the identification of the lesion is possible; 4 points, a small amount of noise around the prostate is observed, but the lesion is clearly visible; and 5 points, almost no noise is seen and the lesion is clearly visible, with a distinct relationship to the prostate.

Our assessment of lesion conspicuity also used the axial T2WI and ADC maps. The evaluation was performed independently and in a blind fashion using a dedicated viewer (VOX-BASE Browser/View; J-Mac system, Sapporo, Japan).

2.3.2. Image analysis: quantitative assessment

For the quantitative assessment, we measured the SNR of the prostate parenchyma and the contrast-to-noise ratio (CNR) of the PCa to prostate parenchyma in both the PI-DWI and DL-DWI images. All of the procedures for the quantitative assessment including the placement of regions of interest (ROIs) were conducted by one board-certified radiologist with 14 years of experience interpreting prostate DWI results, by referring to the axial T2WI with the use of Osirix MD software (ver. 12.5.2; Pixmeo, Geneva, Switzerland).

For the SNR measurement, ROIs drawn by hand were placed on the normal prostate parenchyma and the obturator muscle. The ROI of the normal prostate parenchyma was set to be as large as possible. The ROI of the obturator muscle was set within the right internal obturator muscle at the same level as the prostate. For the CNR measurement, ROIs were placed on the prostate parenchyma and PCa lesion. When multiple PCa lesions were observed in a single case, the ROI was placed on the largest lesion. The ROI of the prostate parenchyma was placed in the same manner as that for the SNR measurement described above. PCa ROIs were placed on hyperintense areas on the DWI images and on the focally hypointense areas on the ADC maps. PCa ROIs were placed on the slice with which the maximum diameter of the abnormal intensity was measured.

For the placement of ROIs for all procedures in the SNR and CNR assessments, the radiologist used the 'copy and paste' function of the software to display five MR images (axial T2WI, PI-DWI, ADC map with PI-DWI, DL-DWI, and ADC map with DL-DWI) in the same window in parallel and thus place identical ROIs in each image.

The methods used to calculate the SNRs and CNRs were as described [14,15]. The SNR was calculated using the following formula:

$$\mathrm{SNR} = \mathrm{SI}_{\text{prostate parenchyma}} / \mathrm{SD}_{\text{obturator muscle}}$$

where $\mathrm{SI}_{\text{prostate parenchyma}}$ is the mean signal intensity in the ROI placed on the prostate parenchyma, and $\mathrm{SD}_{\text{obturator muscle}}$ is the standard deviation in the ROI placed on the obturator muscle.

The CNR was calculated as follows:

$$\mathrm{CNR} = (\mathrm{SI}_{\mathrm{PCa}} - \mathrm{SI}_{\text{prostate parenchyma}}) / \mathrm{SD}_{\text{obturator muscle}}$$

where $\mathrm{SI}_{\mathrm{PCa}}$ is the mean signal intensity in the ROI placed on PCa. The mean ADC values in the ROI of the prostate parenchyma and the PCa were also respectively calculated.

2.4. Histopathological examination

We evaluated all of the radical prostatectomy specimens and biopsy cores, following the guidelines established by the International Society of Urological Pathology (ISUP) [16]. In instances where both a transrectal prostate biopsy and a radical prostatectomy had been conducted at our hospital, we referred to the pathological findings of the radical prostatectomy. When multiple PCa lesions were identified in a single case, we used the highest Gleason score from the largest lesion for the further analysis. In the cases in which the PCa was detected in multiple cores during a transrectal prostate biopsy, we used the highest Gleason score obtained from the ROI corresponding to the delineated lesion on the image.

2.5. Statistical analyses

We compared the qualitative image scores and SNR, CNR, and ADC values obtained by PI-DWI with those obtained by DL-DWI by using the Wilcoxon signed-rank test. Statistical significance was defined as a p-value <0.05. Kappa statistics were used to determine the interobserver agreement for the qualitative analyses, with values falling into the following categories: 0.00–0.20 (poor), 0.21–0.40 (fair), 0.41–0.60 (moderate), 0.61–0.80 (good), and 0.81–1.00 (excellent). The statistical calculations were performed with JMP software (ver. 16.1.0; SAS, Cary, NC, USA).

3. Results

3.1. Patients

A total of 32 male patients with a median age of 73 years (range 58–82 years old) were included in the study. Among them, 14 patients underwent a radical prostatectomy, and the other 18 patients underwent a transrectal prostate biopsy. The Gleason scores for the 32 PCa patients were as follows: 3+3 (n=3 patients), 3+4 (n=5), 4+3 (n=7), 4+4 (n=7), 4+5 (n=7), 5+4 (n=2), and 5+5 (n=1).

3.1.1. Image analysis: qualitative assessment

In the qualitative evaluation, the scores assigned by both of the board-certified radiologists were significantly higher for DL-DWI compared to PI-DWI in all categories, including overall image quality, prostate conspicuity, and lesion conspicuity. The details of the qualitative assessment are summarized in Table 2. There was good

Table 2
Results of the qualitative assessment.

	Reader 1			Reader 2			Kappa-score
	PI-DWI	DL-DWI	p-value	PI-DWI	DL-DWI	p-value	
Overall image quality	3.06 ± 0.67	4.09 ± 0.78	<0.0001	3.03 ± 0.78	3.97 ± 0.90	<0.0001	0.71
Prostate conspicuity	3.09 ± 0.78	4.13 ± 0.75	<0.0001	3.09 ± 0.89	4.16 ± 0.77	<0.0001	0.76
Lesion conspicuity	3.31 ± 0.78	4.28 ± 0.85	<0.0001	3.50 ± 0.80	4.22 ± 0.87	<0.0001	0.69

[footnote] Data are mean ± standard deviation (SD). PI-DWI: DWI with the parallel imaging reconstruction, DL-DWI: DWI with the model-based deep learning reconstruction.

interobserver agreement between the two radiologists in all qualitative analyses, with Kappa scores ranging from 0.69 to 0.76.

3.1.2. Image analysis: quantitative assessment

The mean size of the obturator muscle ROIs was 3.20 ± 0.62 cm^2; that of the normal prostate parenchyma ROIs was 6.17 ± 2.94 cm^2, and that of the PCa ROIs was 2.65± 2.10 cm^2. The SNR, CNR, and ADC values for PI-DWI and DW-DWI are summarized in Table 3. There were significant differences in the SNR and CNR between PI-DWI and DL-DWI (both $p<0.0001$).

The ADC values of both the normal prostate parenchyma and the PCa were significantly higher in DL-DWI than in PI-DWI ($p<0.0001$, $p=0.0014$, respectively). The difference in ADC values between the normal prostate parenchyma and the PCa was significantly larger in DL-DWI compared to PI-DWI ($p<0.0001$). Fig. 1 provides a representative case of PI-DWI and DL-DWI.

4. Discussion

The results of this study demonstrate that the model-based DL reconstruction technique with Adaptive-CS-Net significantly improved the image quality of prostate DWI in both qualitative and quantitative assessments compared to the conventional PI-based technique. This technique enhances the visual quality of prostate DWI by providing high SNRs and CNRs, which can lead to clearer lesion depiction and potentially improve the diagnostic accuracy. This technique may also allow for clearer target recognition in the performance of MRI-US fusion-guided targeted biopsies, leading to more accurate biopsy results and enabling the provision of more suitable treatments for patients. Overall, the model-based DL reconstruction is expected to greatly contribute to the diagnosis of PCa in routine clinical practice.

Although single-shot spin-echo EPI is the most frequently used technique in clinical DWI, combining it with PI methods to reduce geometric image distortions often decreases SNR in regions with high g-factors, particularly in the central area of the image. This decrease in the SNR poses challenges in evaluations of PCa by prostate DWI. Various methods to enhance the image quality of prostate DWI have been explored. Several studies indicated that multi-shot echo-planar imaging (ms-EPI) and readout-segmented echo-planar imaging (rs-EPI) yield better image quality compared to single-shot EPI [17–19]. However, ms-EPI and rs-EPI suffer from the drawback of requiring separate acquisitions for each segment of k-space, leading to prolonged acquisition times with increased k-space segmentation.

Another investigation demonstrated that zoomed DWI results in superior image quality and enhanced lesion conspicuity compared to conventional DWI [20], but imaging by zoomed DWI requires sophisticated equipment, limiting the feasibility of its widespread use.

In this regard, DL-based reconstruction techniques are expected to improve the quality of DWI without extending the acquisition time. Several research groups have recently applied DL-based reconstruction to prostate DWI. Ueda et al. used DL-based reconstruction to enhance the SNR and CNR at high b-values (b=3000 and 5000) in DWI [14]. However, their work focused on image-quality improvement at non-clinical, higher b-values than those routinely used in clinical practice. Ursprung et al. and Johnson et al. reported that applying DL-based reconstruction on DWI acquired with fewer excitations, successfully facilitated a reduction in acquisition times without compromising image quality [21, 22]. However, the primary aim of the research conducted by Ursprung et al. and Johnson et al. was to decrease acquisition times through DL-based reconstruction. In contrast, our present study focused on improving image quality with the use of DL-based reconstruction technique.

Similarly, Lee et al. applied DL-based reconstruction to both standard DWI and DWI with reduced excitations, reporting improvements in SNR and CNR values along with a reduction in image acquisition times [23]. Their findings of image-quality improvement in prostate DWI through DL-based image reconstruction are consistent with our present results.

However, the above-cited studies used 'end-to-end type' DL-based reconstruction in prostate DWI [14,21–23], mainly processing the output image. Conversely, the model-based DL reconstruction approach applied in the present study efficiently utilizes, processes, and integrates large amounts of signal data during iterative image processing, facilitating effective noise reduction [9,10]. This noise reduction method using Adaptive-CS-Net has the potential to achieve superior noise reduction compared to postprocessing- (i.e., end-to-end)-type techniques where only the output image is processed by the CNN.

In the present study, both the prostatic parenchyma and PCa exhibited significantly higher apparent ADC values in DL-DWI compared to PI-DWI. It has been reported that the use of DL-DWI in breast imaging resulted in higher ADC values compared to the use of standard DWI [24], and there are reports indicating no significant difference in ADC values between DL-DWI and conventional DWI in liver imaging [25] as well as reports showing lower ADC values in DL-DWI compared to conventional DWI in liver imaging [26]. The underlying cause(s) of the higher ADC values observed in DL-DWI in our present investigation remain unclear. We speculate that since the level of background noise observed on the prostate gland differed markedly between the DL-DWI and PI-DWI, this resulted in or contributed to the difference of measured ADC values. In our study, the difference in ADC values between prostatic parenchyma and PCa was more pronounced in DL-DWI, potentially enabling radiologists to render a more accurate diagnosis.

Our study has several limitations. We compared DWI using model-based DL reconstruction with DWI based on conventional PI, but we did not compare DWI using model-based DL reconstruction and other

Table 3
Results of the quantitative assessment.

		PI-DWI	DL-DWI	p-value
SNR		16.1 ± 2.8	19.9 ± 3.4	<0.0001
CNR		9.56 ± 5.4	14.9 ± 7.5	<0.0001
ADC, 10^{-6} mm^2/sec	Normal prostate parenchyma	1003 ± 95	1076 ± 112	<0.0001
	Prostate cancer	699 ± 108	716 ± 133	0.0014
	Normal prostate parenchyma – prostate cancer	305 ± 117	360 ± 125	<0.0001

[footnote] Data are mean ± SD. PI-DWI: DWI with the parallel imaging reconstruction, DL-DWI: DWI with the model-based deep learning reconstruction. ADC: apparent diffusion coefficient, CNR: contrast-to- noise ratio, SNR: signal-to-noise ratio.

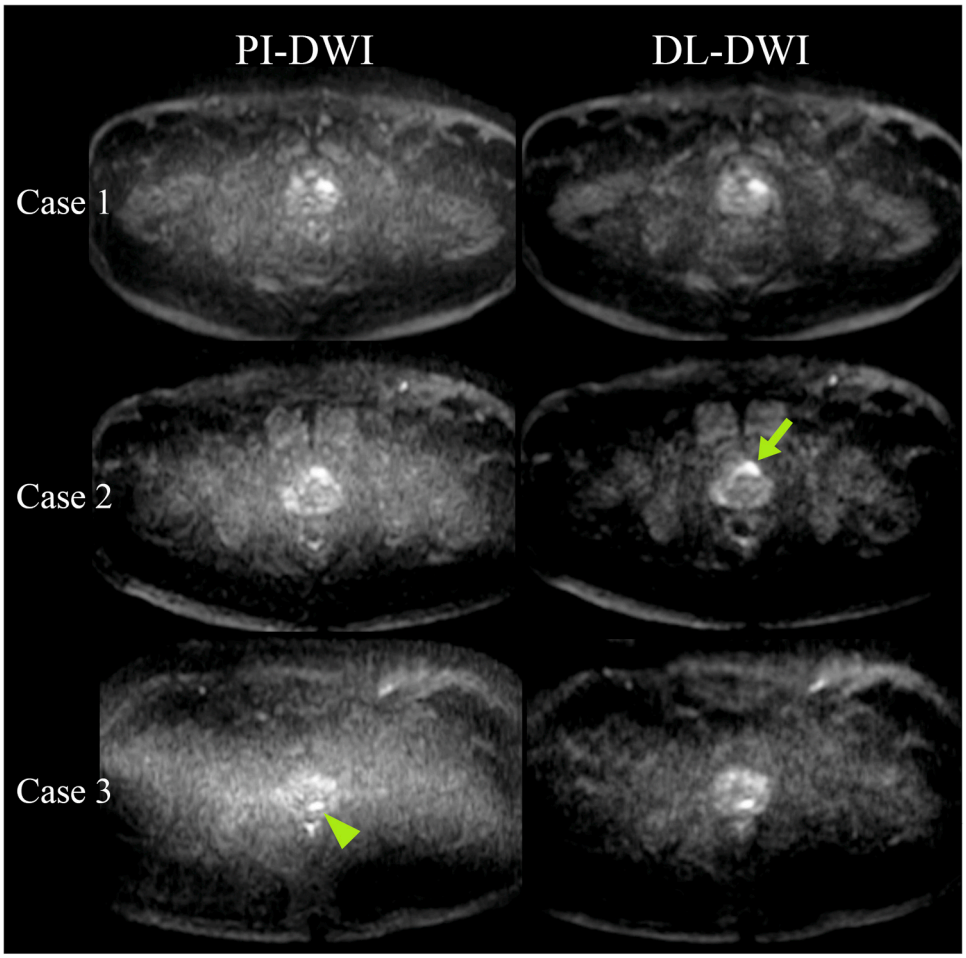

Fig. 1. Representative results of PI-DWI and DL-DWI. The findings of three representative patients with prostate cancer (PCa) examined with both PI- and DL-DWI are presented (Patient 1: *upper row*, Patient 2: *middle row*, and Patient 3: *lower row*). In Patient 1, both PI-DWI and DL-DWI were able to detect PCa, but in DL-DWI only, the anatomical structures in the background were clear due to the marked decrease of the overall noise. In Patient 2, PI-DWI showed moderate noise in the central area on the image, and the outline of the prostate was partially unclear. In this patient's DL-DWI, the image noise observed in the central area was remarkably decreased, and the outline of both the prostate and the PCa (*arrow*) was visible. In Patient 3, PI-DWI presented severe noise in the central area, making the prostate outline barely visible. The lesion, identified as PCa (*arrowhead*), was discernible, though there was considerable noise not associated with the lesion. In the patient's DL-DWI, both the prostate outline and the lesion were clearly identified with an effective decrease of the noise.

DL-based reconstruction methods, especially end-to-end-type methods. Further studies including comparisons of different DL-based reconstruction methods are necessary. The study was also of a relatively small sample size: 32 subjects for the image analysis in a retrospective analysis of patients examined at a single institution. We are keenly aware that a larger sample size could reinforce the validity of our findings. There is a pressing need for prospective, multicenter studies involving larger patient cohorts to overcome this limitation and test the reliability of our results.

5. Conclusion

Our analyses revealed that a model-based DL reconstruction technique enhanced both qualitative and quantitative aspects of image quality in prostate DWI compared to the conventional method, PI-DWI. However, we did not compare this technique with other DL-based methods, particularly end-to-end-type methods, and thus the value of model-based DL reconstruction remains unknown. Despite this limitation, the model-based DL reconstruction technique has the potential to be a valuable tool in the clinical application of prostate DWI by providing clearer lesion depiction.

Funding

This work was supported by a grant from the Japan Society for the Promotion of Science (JSPS) KAKENHI, no. JP21K07558.

Ethical statement

The institutional review board (IRB) of our hospital approved this retrospective study (ID: 022–0388), and the requirement to obtain patients' informed consent was waived. The study was conducted in accord with the ethical standards of the IRB and with the 1964 Helsinki Declaration and its later amendments.

CRediT authorship contribution statement

Hiroshi Kikuchi: Writing – review & editing, Investigation, Data curation. **Masami Yoneyama:** Writing – review & editing, Visualization, Software, Methodology, Formal analysis. **Noriyuki Fujima:** Writing – review & editing, Visualization, Methodology, Formal analysis, Conceptualization. **Jihun Kwon:** Writing – review & editing, Visualization, Software, Methodology, Formal analysis. **Noriko Nishioka:** Writing – original draft, Visualization, Methodology, Formal analysis, Conceptualization. **Takashige Abe:** Writing – review &

editing, Investigation, Data curation. **Ryuji Matsumoto:** Writing – review & editing, Investigation, Data curation. **Keita Sakamoto:** Writing – review & editing, Resources, Investigation. **Rina Kimura:** Writing – review & editing, Resources, Investigation. **Masato Yoshikawa:** Writing – review & editing, Resources, Investigation. **Kohsuke Kudo:** Writing – review & editing, Supervision, Project administration, Conceptualization. **Satonori Tsuneta:** Writing – review & editing, Validation, Resources, Investigation. **Haruka Miyata:** Writing – review & editing, Investigation, Data curation. **Fumi Kato:** Writing – review & editing, Resources, Investigation.

Declaration of Competing Interest

The authors of this manuscript declare relationships with the following companies: Masami Yoneyama and Jihun Kwon are currently employed by Philips Japan. The other authors declare that they have no conflicts of interest.

References

[1] C.M. Hoeks, J.O. Barentsz, T. Hambrock, D. Yakar, D.M. Somford, S.W. Heijmink, T.W. Scheenen, P.C. Vos, H. Huisman, I.M. van Oort, J.A. Witjes, A. Heerschap, J. J. Fütterer, Prostate cancer: multiparametric MR imaging for detection, localization, and staging, Radiology 261 (1) (2011) 46–66.

[2] B. Turkbey, A.B. Rosenkrantz, M.A. Haider, A.R. Padhani, G. Villeirs, K.J. Macura, C.M. Tempany, P.L. Choyke, F. Cornud, D.J. Margolis, H.C. Thoeny, S. Verma, J. Barentsz, J.C. Weinreb, Prostate imaging reporting and data system version 2.1: 2019 update of prostate imaging reporting and data system version 2, Eur. Urol. 76 (3) (2019) 340–351.

[3] J.C. Weinreb, J.O. Barentsz, P.L. Choyke, F. Cornud, M.A. Haider, K.J. Macura, D. Margolis, M.D. Schnall, F. Shtern, C.M. Tempany, H.C. Thoeny, S. Verma, PI-RADS prostate imaging - reporting and data system: 2015, version 2, Eur. Urol. 69 (1) (2016) 16–40.

[4] R. Bammer, S.L. Keeling, M. Augustin, K.P. Pruessmann, R. Wolf, R. Stollberger, H. P. Hartung, F. Fazekas, Improved diffusion-weighted single-shot echo-planar imaging (EPI) in stroke using sensitivity encoding (SENSE), Magn. Reson. Med. 46 (3) (2001) 548–554.

[5] P. Noël, R. Bammer, C. Reinhold, M.A. Haider, Parallel imaging artifacts in body magnetic resonance imaging, Can. Assoc. Radiol. J. 60 (2) (2009) 91–98.

[6] X. Golay, J.A. de Zwart, Y.C. Ho, Y.Y. Sitoh, Parallel imaging techniques in functional MRI, Top. Magn. Reson. Imaging 15 (4) (2004) 255–265.

[7] M.A. Mazurowski, M. Buda, A. Saha, M.R. Bashir, Deep learning in radiology: an overview of the concepts and a survey of the state of the art with focus on MRI, J. Magn. Reson. Imaging 49 (4) (2019) 939–954.

[8] D.J. Lin, P.M. Johnson, F. Knoll, Y.W. Lui, Artificial Intelligence for MR image reconstruction: an overview for clinicians, J. Magn. Reson. Imaging 53 (4) (2021) 1015–1028.

[9] S.Y.Nicola Pezzotti, Mohamed S. Elmahdy, Jeroen van Gemert, Christophe Schülke, Mariya Doneva, Tim Nielsen, Sergey Kastryulin, Boudewijn P.F. Lelieveldt, Matthias J.P. van Osch, Elwin de Weerdt, Marius Staring, An adaptive intelligence algorithm for undersampled Knee MRI reconstruction, IEEE Access 8 (2020).

[10] S.C. Foreman, J. Neumann, J. Han, N. Harrasser, K. Weiss, J.M. Peeters, D. C. Karampinos, M.R. Makowski, A.S. Gersing, K. Woertler, Deep Learning-based Acceleration of Compressed Sense MR imaging of the ankle, Eur. Radiol. 32 (12) (2022) 8376–8385.

[11] X. Wu, L. Tang, W. Li, S. He, X. Yue, P. Peng, T. Wu, X. Zhang, Z. Wu, Y. He, Y. Chen, J. Huang, J. Sun, Feasibility of accelerated non-contrast-enhanced whole-heart bSSFP coronary MR angiography by deep learning-constrained compressed sensing, Eur. Radiol. (2023).

[12] F. Yang, X. Pan, K. Zhu, Y. Xiao, X. Yue, P. Peng, X. Zhang, J. Huang, J. Chen, Y. Yuan, J. Sun, Accelerated 3D high-resolution T2-weighted breast MRI with deep learning constrained compressed sensing, comparison with conventional T2-weighted sequence on 3.0 T, Eur. J. Radiol. 156 (2022) 110562.

[13] N. Fujima, J. Nakagawa, H. Kameda, Y. Ikebe, T. Harada, Y. Shimizu, N. Tsushima, S. Kano, A. Homma, J. Kwon, M. Yoneyama, K. Kudo, Improvement of image quality in diffusion-weighted imaging with model-based deep learning reconstruction for evaluations of the head and neck, Magma (2023).

[14] T. Ueda, Y. Ohno, K. Yamamoto, K. Murayama, M. Ikedo, M. Yui, S. Hanamatsu, Y. Tanaka, Y. Obama, H. Ikeda, H. Toyama, Deep learning reconstruction of diffusion-weighted MRI improves image quality for prostatic imaging, Radiology 303 (2) (2022) 373–381.

[15] J.C. Park, K.J. Park, M.Y. Park, M.H. Kim, J.K. Kim, Fast T2-weighted imaging with deep learning-based reconstruction: evaluation of image quality and diagnostic performance in patients undergoing radical prostatectomy, J. Magn. Reson. Imaging 55 (6) (2022) 1735–1744.

[16] J.I. Epstein, L. Egevad, M.B. Amin, B. Delahunt, J.R. Srigley, P.A. Humphrey, The 2014 International Society of Urological Pathology (ISUP) consensus conference on Gleason grading of prostatic carcinoma: definition of grading patterns and proposal for a new grading system, Am. J. Surg. Pathol. 40 (2) (2016) 244–252.

[17] M. Hosseiny, K.H. Sung, E. Felker, V. Suvannarerg, T. Tubtawee, A. Shafa, K. R. Arora, J. Ching, A. Gulati, A. Azadikhah, X. Zhong, J. Sayre, D. Lu, S.S. Raman, Read-out Segmented Echo Planar Imaging with Two-Dimensional Navigator Correction (RESOLVE): an alternative sequence to improve image quality on diffusion-weighted imaging of prostate, Br. J. Radiol. 95 (1136) () (2022) 20211165.

[18] M. Klingebiel, T. Ullrich, M. Quentin, D. Bonekamp, J. Aissa, D. Mally, C. Arsov, P. Albers, G. Antoch, L. Schimmöller, Advanced diffusion weighted imaging of the prostate: comparison of readout-segmented multi-shot, parallel-transmit and single-shot echo-planar imaging, Eur. J. Radiol. 130 (2020) 109161.

[19] L. Li, L. Wang, M. Deng, H. Liu, J. Cai, V.K. Sah, J. Liu, Feasibility study of 3-T DWI of the prostate: readout-segmented versus single-shot echo-planar imaging, AJR Am. J. Roentgenol. 205 (1) (2015) 70–76.

[20] L. Hu, L. Wei, S. Wang, C. Fu, T. Benker, J. Zhao, Better lesion conspicuity translates into improved prostate cancer detection: comparison of non-parallel-transmission-zoomed-DWI with conventional-DWI, Abdom. Radiol. 46 (12) (2021) 5659–5668.

[21] S. Ursprung, J. Herrmann, N. Joos, E. Weiland, T. Benkert, H. Almansour, A. Lingg, S. Afat, S. Gassenmaier, Accelerated diffusion-weighted imaging of the prostate using deep learning image reconstruction: a retrospective comparison with standard diffusion-weighted imaging, Eur. J. Radiol. 165 (2023) 110953.

[22] P.M. Johnson, A. Tong, A. Donthireddy, K. Melamud, R. Petrocelli, P. Smereka, K. Qian, M.B. Keerthivasan, H. Chandarana, F. Knoll, Deep learning reconstruction enables highly accelerated biparametric MR imaging of the prostate, J. Magn. Reson. Imaging 56 (1) (2022) 184–195.

[23] K.L. Lee, D.A. Kessler, S. Dezonie, W. Chishaya, C. Shepherd, B. Carmo, M. J. Graves, T. Barrett, Assessment of deep learning-based reconstruction on T2-weighted and diffusion-weighted prostate MRI image quality, Eur. J. Radiol. 166 (2023) 111017.

[24] C. Wilpert, C. Neubauer, A. Rau, H. Schneider, T. Benkert, E. Weiland, R. Strecker, M. Reisert, M. Benndorf, J. Weiss, F. Bamberg, M. Windfuhr-Blum, J. Neubauer, Accelerated diffusion-weighted imaging in 3 T breast MRI using a deep learning reconstruction algorithm with superresolution processing: a prospective comparative study, Investig. Radiol. (2023).

[25] D.H. Kim, B. Kim, H.S. Lee, T. Benkert, H. Kim, J.I. Choi, S.N. Oh, S.E. Rha, Deep Learning-ACcelerated Liver Diffusion-weighted Imaging: Intraindividual Comparison and Additional Phantom Study of Free-breathing and Respiratory-triggering Acquisitions, Invest Radiol. 58 (11) (2023) 782–790.

[26] S.H. Bae, J. Hwang, S.S. Hong, E.J. Lee, J. Jeong, T. Benkert, J. Sung, S. Arberet, Clinical feasibility of accelerated diffusion weighted imaging of the abdomen with deep learning reconstruction: comparison with conventional diffusion weighted imaging, Eur. J. Radiol. 154 (2022) 110428.